Static thermodynamic properties of the linear half-filled-band Hubbard model*

W. A. Seitz
Department of Chemistry, The University of Texas at Austin, Austin, Texas 78712

D. J. Klein
Department of Physics, The University of Texas at Austin, Austin, Texas 78712

(Received 12 September 1973)

Low-temperature static thermodynamic properties of the linear half-filled-band Hubbard model are computed via a numerical-perturbative method which applies near the atomic limit. Curves for the internal energy, entropy, specific heat, and magnetic susceptibility are reported.

I. INTRODUCTION

Suggestions[1-3] that some aromatic donor-acceptor salts are reasonably described by a linear half-filled-band Hubbard model have contributed to the interest in the finite-temperature properties of this model. The regime of this experimental interest is near the atomic limit of the Hubbard model and corresponds to low temperatures, in comparison to the parameters appearing in the model Hamiltonian. Especially in this regime of present interest, reliable thermodynamic properties have been difficult to obtain. Exact zero-temperature treatments, self-consistent-field (SCF) and random-phase-approximation (RPA) solutions, functional-integral approaches, and high-temperature-series expansions have all been applied but have not achieved the desired reliability, as discussed elsewhere.[4,5] Exact numerical calculations on finite Hubbard chains have previously[6-8] been ambiguous in extrapolation to infinite chain lengths. A second-order perturbation expansion[9] about the atomic limit has related the Hubbard-model properties to those of a simple Heisenberg model for which, in turn, reliable results are available.[10]

Here we report results involving an extension of the perturbation expansion to sixth order, followed by numerical finite-chain calculations. Extrapolation to infinite perturbation order followed by extrapolation to infinite chain length yields what we believe are the best estimates of the actual Hubbard-model thermodynamic properties within the regime of interest indicated above. Extrapolated results for the internal energy, specific heat, entropy, and zero-field magnetic susceptibility are reported.

The N-site linear Hubbard model is broken into zero-order and perturbation terms:

$$H \equiv H^0 + V \quad ,$$

$$H^0 \equiv I \sum_{n=1}^{N} a_{n\alpha}^{\dagger} a_{n\alpha} a_{n\beta}^{\dagger} a_{n\beta} \quad , \tag{1.1}$$

$$V \equiv \Delta \sum_{n=1}^{N} \sum_{\sigma} (a_{n\sigma}^{\dagger} a_{(n+1)\sigma} + a_{(n+1)\sigma}^{\dagger} a_{n\sigma}) \quad ,$$

where $a_{n\sigma}^{\dagger}$ and $a_{n\sigma}$ are fermion creation and annihilation operators for an orbital of spin σ on site n. Since for the regime of interest the charge-transfer integral Δ is much less than the intrasite Coulomb-repulsion integral I, a perturbation expansion suggests itself. Degenerate perturbation theory yields[4] an effective Hamiltonian defined on the N-electron zero-order ground-state eigenspace,

$$\mathcal{H} = \left(-\frac{2\Delta^2}{I} + \frac{8\Delta^4}{I^3} - \frac{40\Delta^6}{I^5}\right) A_1 + \left(-\frac{2\Delta^4}{I^3} + \frac{12\Delta^6}{I^5}\right) A_2 + \left(-\frac{2\Delta^6}{I^5}\right) B + (\text{eighth- and higher-order terms}), \tag{1.2}$$

where

$$A_1 \equiv \sum_n [1 - (n, n+1)] = \sum_n \left(\frac{1}{2} - 2\vec{S}_n \cdot \vec{S}_{n+1}\right) \quad ,$$

$$A_2 \equiv \sum_n [1 - (n, n+2)] \quad , \tag{1.3}$$

$$B \equiv \sum_n [1 - (n, n+1)(n+2,\ n+3) + (n, n+2) \times (n+1,\ n+3) - (n, n+3)(n+1,\ n+2)] \quad .$$

TABLE I. Ground-state energies per site accurate through second, fourth, and sixth orders for 11- and 12-site chains. Energies are given in units of $J = 2\Delta^2/I$, and the last column gives the value extrapolated to infinite perturbation order.

N	Δ/I	$E^{(2)}/NJ$	$E^{(4)}/NJ$	$E^{(6)}/NJ$	$E^{(\infty)}/NJ$
11	0.05	−1.35798	−1.34483	−1.34500	−1.34497
	0.10	−1.35798	−1.30537	−1.30811	−1.30766
	0.15	−1.35798	−1.23964	−1.25349	−1.25062
	0.20	−1.35798	−1.14766	−1.19139	−1.18066
12	0.05	−1.39790	−1.38423	−1.38441	−1.38438
	0.10	−1.39790	−1.34323	−1.34606	−1.34561
	0.15	−1.39790	−1.27493	−1.28924	−1.28635
	0.20	−1.39790	−1.17935	−1.22455	−1.21304

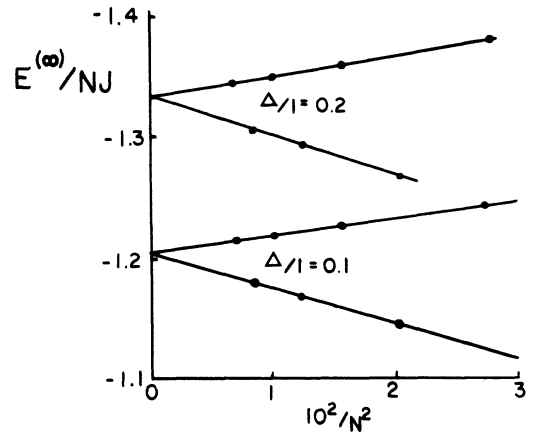

FIG. 1. Ground-state energies per site, $E^{(\infty)}$, for finite chains (in units of $J=2\Delta^2/I$) vs $1/N^2$ for $\Delta/I=0.1$ and 0.2. The even- and odd-chain values lie on straight lines which meet at $1/N^2=0$, corresponding to infinite chains.

This effective Hamiltonian is defined on the 2^N-dimensional space of N-electron spin kets. Hence $\mathcal{H}$ is a generalized effective Heisenberg spin Hamiltonian. Consideration of only the single zero-order eigenspace is expected to be justified so long as we confine ourselves to temperatures small compared to the energy I of the first excited zero-order eigenspace. Further, since this zero-order eigenspace has a dimension much less than that for the full Hubbard model, numerical solutions for longer finite chains can be made.

II. FINITE-CHAIN CALCULATIONS AND EXTRAPOLATION TO INFINITE PERTURBATION ORDER

We have carried out finite-cyclic-chain computations on the Hamiltonian of Eq. (1.2) truncated at second, fourth, and sixth orders and for Δ/I values of 0.05, 0.10, 0.15, and 0.20. The limiting factor in such calculations is the size of the matrices involved and the computer time available. Thus Bonner and Fisher[10] computed for cyclic Heisenberg chains up to length $N=11$, while Shiba and Pincus[6] computed for cyclic Hubbard chains up to length $N=6$. Here we compute for chains up to length $N=12$, and expect, in consequence of Bonner and Fisher's experience, [10] that this should make possible somewhat more reliable extrapolation than using just chains up to $N=6$. The details of the computational technique which employ full point-group, permutation, and spin-symmetry factorizations are described elsewhere. [11]

Solving the second-, fourth-, and sixth-order truncated effective Hamiltonians, we obtain energies $E_i^{(2)}$, $E_i^{(4)}$, $E_i^{(6)}$ accurate through these respective orders. The ground-state energies per site

TABLE II. Ground-state energies per site (in units of J): (a) exact result for the Heisenberg-model chain (corresponding to second order), E_{Heis}; (b) simple average of the infinite-perturbation-order $N=11$ and $N=12$ results, $\overline{E}_A$; (c) extrapolated result as in Fig. 1, $\overline{E}$; (d) exact Hubbard-model result of Lieb and Wu, E_{Hub}.

Δ/I	E_{Heis}/NJ	$\overline{E}_A/NJ$	$\overline{E}/NJ$	E_{Hub}/NJ
0.05	−1.3863	−1.3647	−1.3726	−1.3705
0.10	−1.3863	−1.3266	−1.3342	−1.3359
0.15	−1.3863	−1.2685	−1.2756	−1.2812
0.20	−1.3863	−1.1966	−1.2031	−1.2163

are given in Table I in units of $J\equiv 2\Delta^2/I$. As expected, convergence is best for low values of Δ/I, but even at $\Delta/I=0.20$ convergence appears good.

The extrapolation of second-, fourth-, and sixth-order eigenvalues $E_i^{(2)}$, $E_i^{(4)}$, and $E_i^{(6)}$ to give an estimate of the corresponding infinite-order eigenvalue $E_i^{(\infty)}$ is obtained by a least-squares fit to the expression

$$E_i^{(2n)}=\epsilon_i^{(2)}\sum_{j=0}^{n-1}x_i^j \tag{2.1}$$

(we note[4] the absence of odd perturbation order). From the least-squares values of $\epsilon_i^{(2)}$ and x_i we obtain the infinite-order estimate

$$E_i^{(\infty)}=\epsilon_i^{(2)}/(1-x_i) \quad . \tag{2.2}$$

These infinite-order estimates for the ground state are also reported in Table I. This extrapolation

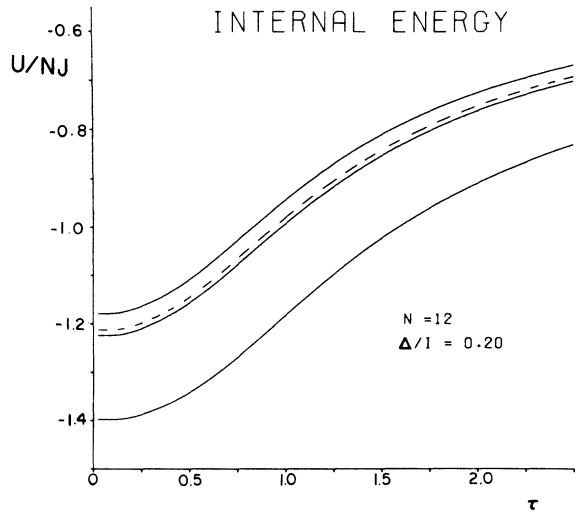

FIG. 2. Internal energy per site for $N=12$ with $\Delta/I=0.2$. The dashed curve is computed from the infinite-perturbation-order eigenvalues, while those computed from the sixth-, fourth-, and second-order eigenvalues are progressively more distant.

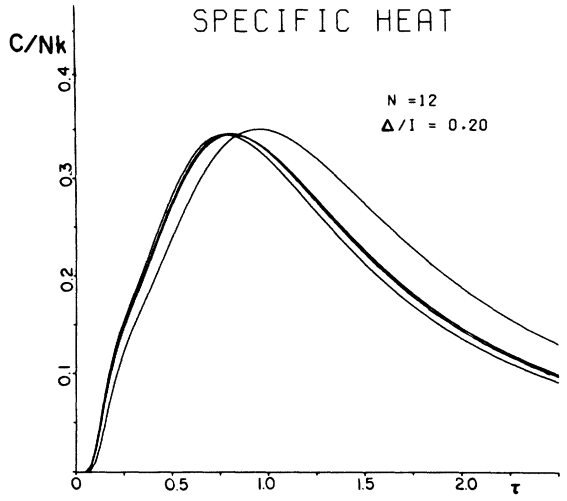

FIG. 3. Specific heat site for $N=12$ with $\Delta/I=0.2$. The infinite-order curve is the lower of the two closely spaced curves at large τ, with the curves for sixth, fourth, and second order progressively more distant.

is made for all energy levels to obtain the final estimates of the infinite-order perturbed energy levels for use in the computations of thermodynamic properties. We note that the maximum use of available symmetries helps us in identifying the corresponding eigenvalues in different orders of perturbation.

A further indication of the accuracy of these extrapolated infinite-perturbation-order eigenvalues may be obtained by extrapolation of the finite-chain ground-state energies to infinite chain length and comparison with the exact results of Lieb and Wu.[12] The extrapolation to infinite chain length may be accomplished by plotting these energies versus $1/N^2$. Such plots for $\Delta/I=0.1$ and 0.2 are given in Fig. 1 and are found to be linear for even and odd chains, as was the case for the Heisenberg model.[10] These infinite-chain Hubbard-model ground-state extrapolations are reported in Table II, and they are compared to the average of $N=11$ and 12 energies, the exact Heisenberg-model values,[13] and the exact Hubbard-model values.[12] There is a small error in the extrapolated results ranging from about 0.15 to 1.1% of the magnitude of the energy. However, even for $\Delta/I=0.2$ the extrapolation gives a significant improvement over the second-order Heisenberg-model result.

III. THERMODYNAMIC PROPERTIES AND EXTRAPOLATION TO INFINITE CHAIN LENGTH

Finite-chain thermodynamic functions were obtained in the canonical ensemble by direct computation of Boltzmann averages, just as Bonner and Fisher[10] did. The results are reported in terms of energy units of $J\equiv 2\Delta^2/I$ and of reduced temperature $\tau\equiv k_BT/J$.

The thermodynamic properties were computed using perturbation energies accurate through the various perturbation orders. The second-order curves thus reproduce the simple Heisenberg-model properties. Figure 2 shows the temperature dependence of these different perturbation-order internal energies per site as computed for a chain with $N=12$ and $\Delta/I=0.2$. Even for this largest value of Δ/I the convergence to infinite perturbation order appears good. Curves for entropy, specific heat, and magnetic susceptibility show even better convergence. Figure 3 shows the specific heat per site for the same chain as in Fig. 2. Here the second-order Heisenberg-model curve is modified by a decrease and shift to lower temperatures of the maximum; further, the low-temperature slope increases. For the magnetic susceptibility the second-order Heisenberg-model curve is modified by an increase and shift to lower temperatures of the maximum.

Given the infinite-perturbation-order properties for finite chains, we wish to extrapolate to infinite-system properties. We define an *iterated* mean for a property P, with value P_N for chains of length N,

$$I_N\equiv A_N^{(\infty)}=G_N^{(\infty)} \quad , \tag{3.1}$$

where $A_N^{(\infty)}$ and $G_N^{(\infty)}$ are limits of the arithmetic and geometric means,

$$\begin{aligned} A_N^{(n)}&\equiv\tfrac{1}{2}(A_N^{(n-1)}+G_N^{(n-1)}),\quad n\geq 1\\ G_N^{(n)}&\equiv(A_N^{(n-1)}G_N^{(n-1)})^{1/2},\quad n\geq 1\end{aligned} \tag{3.2}$$

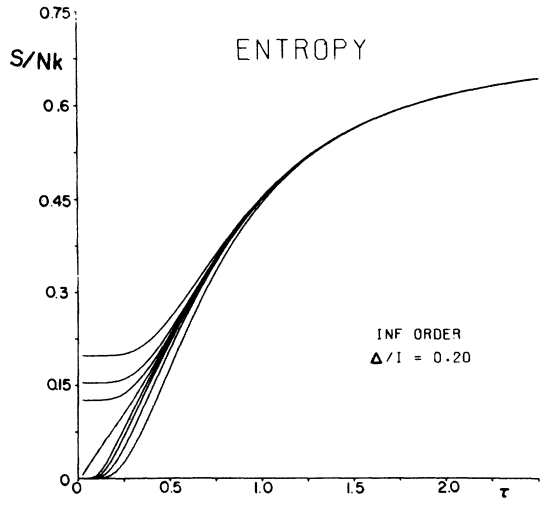

FIG. 4. Entropy per site curves for $N=6-12$ and $\Delta/I=0.2$ showing the infinite-chain extrapolation approaching $\tau=0$ with nonzero slope. The even chains approach from below and the odd chains from above with increasing N.

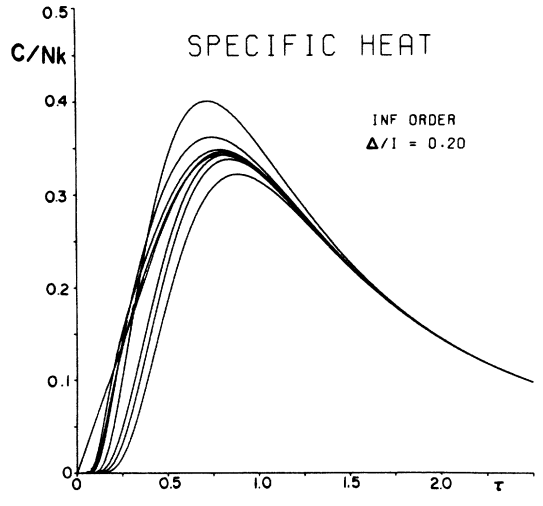

FIG. 5. Specific heat per site for $N=6-12$ and $\Delta/I=0$. showing the infinite-chain extrapolation approaching $\tau=0$ with nonzero slope. The maximum decreases with increasing N for even chains while increasing for odd N.

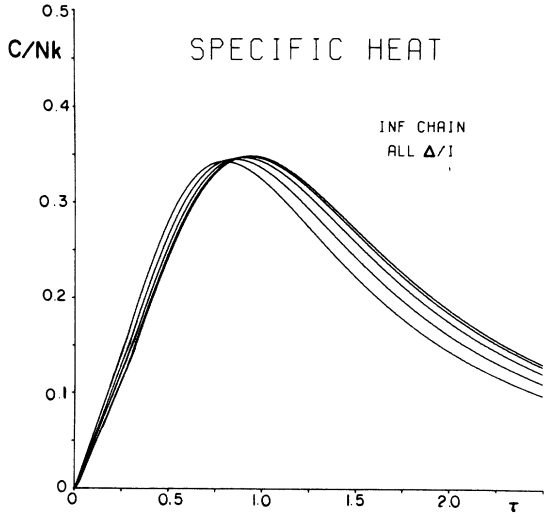

FIG. 7. Specific heat per site for infinite chains. At high temperatures the Heisenberg-model result lies highest with the values for $\Delta/I=0.05$, 0.10, 0.15, and 0.20 progressively lower. Note, though, at low temperatures this order is reversed with the low-temperature slope larger for larger Δ/I.

and where

$$A_N^{(0)} \equiv \tfrac{1}{2}(P_N+P_{N+1}) \quad , \qquad G_N^{(0)} \equiv (P_N P_{N+1})^{1/2} \quad . \tag{3.3}$$

Having obtained the set of iterated means $\{I_6, I_7, \ldots, I_{11}\}$ for property P at temperature τ, we least-squares fit these values, as a function of both $1/N$ and $1/N^2$, to two straight lines, one line for even N and one for odd N, such that the corresponding even and odd lines have the same value as $N\to\infty$. This line fitting is similar to that displayed for the ground-state energy in Fig. 1. The $N\to\infty$ values, say, a and a', and least-squares errors, say, ϵ and ϵ', obtained on considering the I_N as functions of $1/N$ and $1/N^2$, respectively, are then combined to give our final infinite-chain esti-

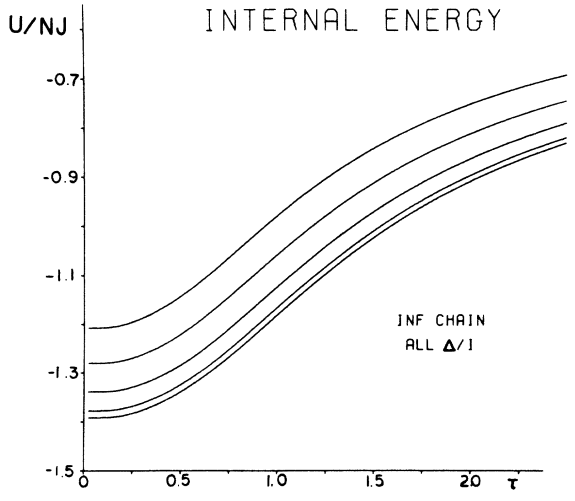

FIG. 6. Internal energy per site for infinite chains for $\Delta/I=0$, 0.05, 0.10, 0.15, and 0.20. The Heisenberg-model curve lies lowest with the value increasing with Δ/I.

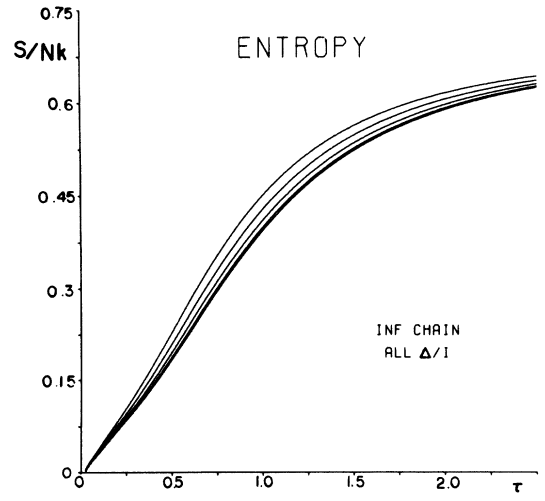

FIG. 8. Entropy per site for infinite chains for $\Delta/I=0.0$, 0.05, 0.10, 0.15, and 0.20. The zero-temperature slope is again seen to increase with Δ/I.

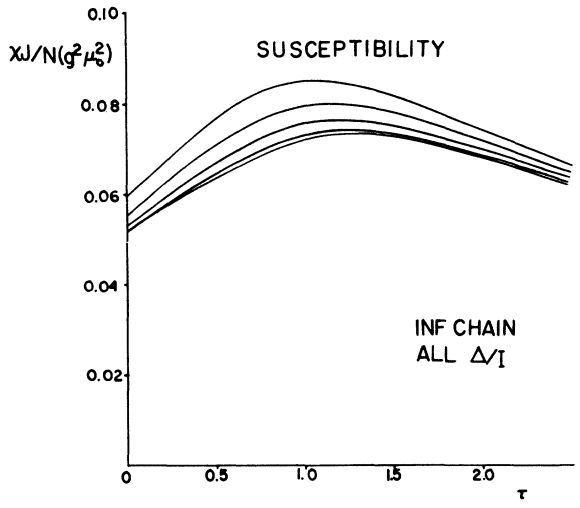

FIG. 9. Magnetic susceptibilities for all Δ/I. The maximum increases and moves to lower temperatures as Δ/I increases. The zero-temperature limits are exact (Ref. 14).

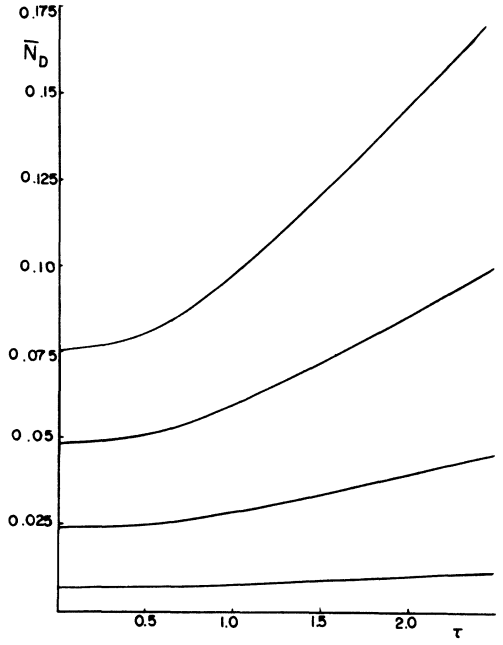

FIG. 10. Average number of doubly occupied sites as a function of temperature for $\Delta/I = 0.05$, 0.1, 0.15, and 0.2. The value of $\bar{N}_D$ increases with both temperature and Δ/I.

mate for the property P,

$$\bar{P} \equiv \frac{a\epsilon' + a'\epsilon}{\epsilon + \epsilon'} \quad . \tag{3.4}$$

This general procedure has some desirable features found in practice. The iterated mean is intermediate between the simple harmonic and arithmetic means, often yielding more reasonable results than either of these simple means. The dual line fitting arises because of the different behavior of odd- and even-chain properties. Finally, some finite-chain properties deviate from the infinite-chain results by errors primarily of order $1/N^2$ (as the ground-state energy), while others also have important errors of order $1/N$.

The curves for the entropy per site for chain lengths $N = 6-12$ and the infinite-length-chain extrapolation are shown in Fig. 4. We see that the infinite-chain extrapolation appears to be more accurate at the lower temperatures than simple harmonic or arithmetic means (which would tend towards the $N = 12$ curve or one-half the $N = 11$ curve, respectively). The results for the specific heat appear less well converged at low temperatures; however, employing the apparently well-converged entropy curve, one may generate, as described by Bonner and Fisher,[10] the low-temperature slope of the specific-heat curve. Coupling this low-temperature slope with our methodically extrapolated results at higher temperatures gives the infinite-chain estimate of Fig. 5. Finite-chain results are also shown. Also, in the case of the magnetic susceptibility the exact[14] zero-temperature value is coupled with our methodically extrapolated results at higher temperatures.

In Figs. 6–9 the fully extrapolated thermodynamic properties are shown for $\Delta/I = 0.00$, 0.05, 0.10, 0.15, and 0.20. It is seen that the Hubbard-model properties incorporating higher-order perturbation effects are similar to those of the second-order Heisenberg model; however, there are important quantitative modifications. As Δ/I increases all the properties increase in value except for the low-temperature specific heat. Also as Δ/I increases the maxima in the specific-heat and magnetic-susceptibility curves shift to lower temperatures. In Table III we give our estimates of the location and magnitude of the maxima for the susceptibility and specific-heat curves, as well as the zero-temperature slope of the entropy.

TABLE III. Selected data for extrapolated infinite-order infinite-chain properties.

Δ/I	$\chi_{max} J/Ng^2\mu^2$	τ_{max}	C_{max}/Nk	τ_{max}	$(1/Nk)/(\partial S/\partial\tau)_{\tau=0}$
0.0	0.0734	1.26	0.349	0.93	3.45
0.05	0.0743	1.26	0.349	0.93	3.49
0.10	0.0765	1.21	0.348	0.90	3.62
0.15	0.0802	1.15	0.346	0.85	3.84
0.20	0.0852	1.07	0.344	0.80	4.16

In some discussions[2] of the properties of the Hubbard model the average density of doubly occupied sites has played a role. We have also computed this quantity, using the formula

$$\bar{N}_D = \frac{\partial F}{\partial I} \quad , \tag{3.5}$$

where F is the free energy per site. This was obtained by least-squares fitting the values of F/Δ for the various Δ/I at a given reduced temperature τ to a quadratic in Δ/I. The resulting polynomial was then differentiated with respect to I to obtain the result for $\bar{N}_D$ at temperature τ. The results of this computation are given in Fig. 10. The zero-temperature results agree closely with the ones[6] obtained from the exact zero-temperature free energy of Lieb and Wu.

IV. CONCLUSION

We have computed the low-temperature static thermodynamic properties of the linear half-filled-band Hubbard model via a numerical-perturbative technique. These results should provide an accurate low-temperature picture near the atomic limit ($\Delta \ll I$). The low-temperature regime of accuracy can be estimated by considering the excitation energy from the Hubbard-model ground state to the lowest state arising from the zero-order eigenspaces we have presently neglected. This "single-particle excitation" energy is smallest (in units of Δ) for larger Δ/I, and it takes[15] a value of $\sim 2\Delta$ at $\Delta/I = 0.20$, so that the low-temperature regime is $\tau \ll 2\Delta$. Another estimate is obtained on comparing finite-Hubbard-model-chain calculations[6] with our finite-chain Heisenberg-model calculations. This comparison suggests that our results are accurate to $\lesssim 10\%$ for values of $\tau J \cong \Delta/2$ with very rapid increase in accuracy for smaller τJ. Coupling our results with recent high-temperature results[16] for the linear half-filled-band Hubbard model thus provides reliable data for the static thermodynamic properties in the atomic limit.

---

*Research supported by the Robert A. Welch Foundation.

[1](a) P. J. Strebel and Z. G. Soos, J. Chem. Phys. 53, 4077 (1970); (b) D. J. Klein and Z. G. Soos, Mol. Phys. 20, 1013 (1971); (c) Z. G. Soos and A. J. Silverstein, Mol. Phys. 23, 775 (1972).

[2](a) A. J. Epstein, S. Etemad, A. F. Garito, and A. J. Heeger, Solid State Commun. 9 1803 (1971); (b) Phys. Rev. B 5, 952 (1972).

[3](a) A. N. Bloch, R. B. Weisman, and C. M. Varma, Phys. Rev. Lett. 28, 752 (1972); (b) E. Ehrenfreund, S. Etemad, L. B. Coleman, E. F. Rybaczewski, A. F. Garito, and A. J. Heeger, Phys. Rev. Lett. 29, 269 (1970); (c) E. Ehrenfreund, E. F. Rybaczewski, A. F. Garito, and A. J. Heeger, Phys. Rev. Lett. 28, 873 (1972).

[4]D. J. Klein and W. A. Seitz, Phys. Rev. B 8, 2236 (1973).

[5]J. H. Choi and W. R. Thorson, J. Chem. Phys. 57 252 (1970).

[6](a) H. Shiba and P. A. Pincus, Phys. Rev. B 5, 1966 (1972); (b) H. Shiba, Prog. Theor. Phys. 48, 2171 (1972).

[7](a) K. H. Heinig and J. Monecke, Phys. Status Solidi (b) 49, K139 (1972); (b) Phys. Status Solidi; (b) 49, K141 (1972); (c) K. H. Heinig and J. Monecke, Phys. Status Solidi (b) 50, K117 (1972).

[8]D. Cabib and T. A. Kaplan, Phys. Rev. B 7, 2199 (1973).

[9](a) P. W. Anderson, Phys. Rev. 115, 2 (1959); (b) L. N. Buleavski, Zh. Eksp. Teor. Fiz. 51, 230 (1966) [Sov. Phys.–JETP 24, 154 (1967)]; (c) J. H. Van Vleck, in *Quantum Theory of Atoms, Molecules and the Solid State*, edited by P. O. Löwdin (Academic, New York, 1966), p. 475.

[10](a) J. C. Bonner and M. E. Fisher, Phys. Rev. 135, A640 (1964); (b) J. C. Bonner, doctoral dissertation (University of London, 1968) (unpublished).

[11](a) W. A. Seitz and D. J. Klein, Intern. J. Quantum Chem. 7, 647 (1973); (b) W. A. Seitz, doctoral dissertation (University of Texas, 1973) (unpublished).

[12]E. H. Lieb and F. Y. Wu, Phys. Rev. Lett. 20, 1445 (1968).

[13](a) H. Bethe, Z. Phys. 71, 209 (1931); (b) L. Hulthen, Arkiv Mat. Astron. Fysik. 26A, 1 (1938).

[14]M. Takahashi, Prog. Theor. Phys. 42, 1098 (1969); Prog. Theor. Phys. 43, 1619 (1970).

[15]A. A. Ovchinnikov, Zh. Eksp. Teor. Fiz. 57, 2137 (1969) [Sov. Phys.–JETP 30, 1160 (1970)].

[16](a) D. W. Hone and P. Pincus, Phys. Rev. B 7, 4889 (1973); (b) P. B. Visscher (unpublished).